ORIGINAL ARTICLE

Adjudin synergizes with paclitaxel and inhibits cell growth and metastasis by regulating the sirtuin 3–Forkhead box O3a axis in human small-cell lung cancer

Xue Wang[1*], Qingyu Zeng[2*], Ziming Li[1*], Xiao Yang[2], Weiliang Xia[2] & Zhiwei Chen[1] (iD)

1 Shanghai Lung Cancer Center, Shanghai Chest Hospital, Shanghai Jiao Tong University, Shanghai, China
2 School of Biomedical Engineering and Med-X Research Institute, Shanghai Jiao Tong University, Shanghai, China

Correspondence
Weiliang Xia, State key Laboratory of Oncogenes and Related Genes, School of Biomedical Engineering and Med-X Research Institute, Shanghai Jiao Tong University, Huashan Road 1954, Shanghai 200030, China.
Tel: +86 21 6293 3351; +86 13 5858 87951
Fax: +86 21 62932302
Email: wlxia@sjtu.edu.cn

Zhiwei Chen, Shanghai Lung Cancer Center, Shanghai Chest Hospital, Shanghai Jiao Tong University, West Huaihai Road 241, Shanghai 20030, China.
Tel: +86 180 1732 1552
Fax: 22200000-3401
Email: czw75@shchest.org

*These authors contributed equally to this work

Abstract

Background: Small-cell lung cancer (SCLC), a malignant tumor, is usually widely metastatic when diagnosed. The lack of important therapeutic clinical advances makes it difficult to treat. Previous studies showed that Adjudin had anticancer effects in many other human cancers, and it was synergetic with cisplatin in non-small cell lung cancer. However, the mechanism on SCLC was unclear.

Methods: We investigated the potential mechanism and effect of Adjudin on SCLC both *in vitro* and *in vivo*.

Results: An SCLC xenograft model showed that Adjudin inhibited tumor growth and was significantly synergetic with paclitaxel (*in vitro* as well). Cell Counting Kit-8 assays, flow cytometric analysis and western blotting showed that Adjudin effectively suppressed SCLC cell proliferation by inducing S phase arrest and caspase-dependent apoptosis. Moreover, Transwell and scratch assays showed that Adjudin also effectively inhibited migration and invasion. Furthermore, Adjudin activated the sirtuin 3 (SIRT3)–Forkhead box O3a (FOXO3a) pathway. Downregulating SIRT3 or FOXO3a significantly attenuated Adjudin-induced anticancer effects. Furthermore, higher expression of SIRT3 and FOXO3a were positively correlated, and both were associated with longer survival in lung cancer patients.

Conclusion: Overall, the present study is the first to show that Adjudin synergizes with paclitaxel and inhibits cell growth and metastasis by regulating the SIRT3–FOXO3a axis in SCLC; thus, Adjudin has great potential to be an anticancer agent.

Introduction

In recent years, the incidence of lung cancer has grown rapidly,[1] and it is the most common cause of cancer-related death. There are two classes of lung cancer: small cell lung cancer (SCLC) and non-small cell lung cancer (NSCLC). SCLC represents approximately 15% of all lung cancer cases, with a 7% five-year survival rate.[2,3] Since the 1980s, systemic chemotherapy with a platinum and etoposide combination remains the most commonly used frontline treatment of extensive-stage SCLC. Although response rates to first-line therapy are extremely high (approximately 60–65%), patients' outcomes remain poor (a modest median overall survival of approximately 10 months).[4–6] Doctors have no available treatments for those patients, so it is critical to identify new targets to help those who are suffering from SCLC.

Figure 1 Adjudin displayed good anticancer activity in human small-cell lung cancer cell lines. (**a**) The chemical structure of Adjudin. (**b**) Cell viability of NCI-H446 or DMS114 cells was examined by Cell Counting Kit-8 assay as described after being treated with different concentrations of Adjudin (0, 20, 40, 60, 80, 100 μM) for up to 72 hours (■) 24 hours, (▨) 48 hours, and (▢) 72 hours (one-way ANOVA test). (**c**) Scratch and (**d**) Transwell assays were conducted to access cell migration and invasion after cells were treated with Adjudin (40 μM) or vehicle (dimethyl sulfoxide) for 24 hours (one-way ANOVA test). (**e**) NCI-H446 and DMS114 cells were treated with or without Adjudin (40 μM) for 24 hours, and then EMT-related proteins (E-cadherin, N-cadherin, and vimentin) were analyzed by western blotting (Student's *t*-test). Data were representative of three independent experiments. Data are presented as the mean ± SD of triplicate experiments; *$P < 0.05$; **$P < 0.01$; ***$P < 0.001$; ****$P < 0.0001$; scale bar, 100 μm. (■) Vehicle, and (▨) Adjudin (μM)
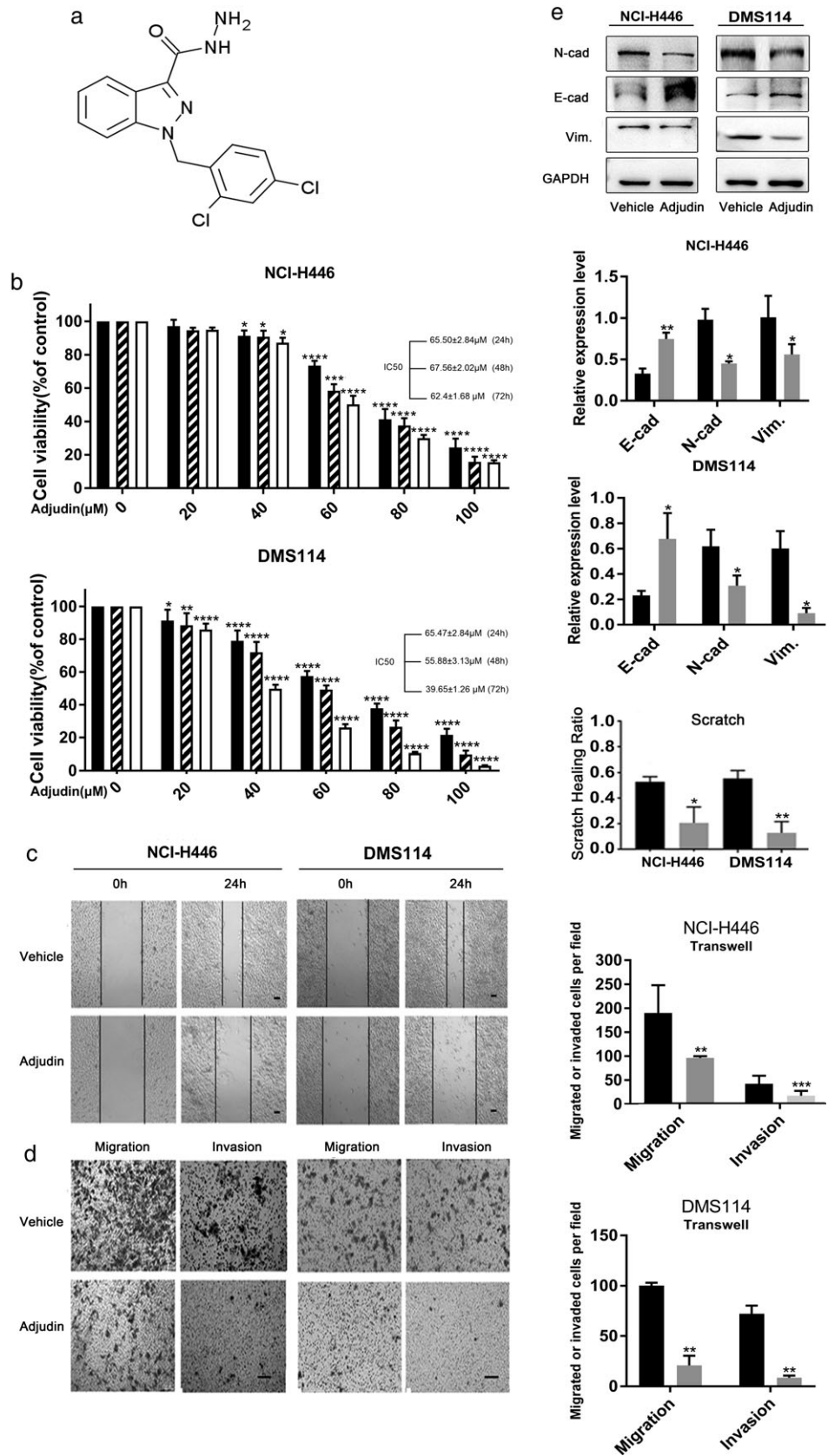
Adjudin (AF-2364; Fig 1a), a potential non-hormonal male contraceptive drug,[7–10] mediates adherens junction disruption at the Sertoli-germ cell interface and is a potential non-hormonal male contraceptive.[8,11–14] Recently, studies have found that it also plays significant roles in other fields, such as ischemia stroke,[15] multidrug-resistant cancers,[16] prevention of gentamicin ototoxicity,[17] and anti-cancer.[2] Our predecessors found that Adjudin had anticancer effects in prostate cancer, glioma, and NSCLC.[2] However, its effect on SCLC has never been studied, so thorough research should be carried out.

Sirtuin 3 (SIRT3), one of the NAD$^+$-dependent deacetylases[18] that regulates cellular proliferation and differentiation, metabolism, and response to stress, has been reported as a therapeutic target in cancer.[18–20] Forkhead box O3 (FOXO3a,), also known as FOXO3, is a human protein encoded by the *FOXO3* gene; it has effects on DNA repair, which may regulate the resistance of cells to stress and affect the lifespan of the organism.[21] However, how SIRT3 and FOXO3a work in SCLC has never been studied.

In the current study, we first reported that Adjudin synergizes with paclitaxel and functions in SCLC through the SIRT3–FOXO3a axis.

Methods

Cell culture and reagents

NCI-H446 and DMS114 (human SCLC) cell lines purchased from ATCC (Rockefeller, MY, USA) were cultured in RPMI-1640 (HyClone, Logan, UT, USA) supplemented with 10% fetal bovine serum (FBS; Gemini, West Sacramento, CA, USA), 100 U/mL penicillin, and 100 μg/mL streptomycin (Invitrogen, Carlsbad, CA, USA). They were incubated at 37°C in an atmosphere of 5% CO2. Adjudin was provided by Dr C Yan Cheng of the Mary M Wohlford Laboratory, Population Council, New York, USA. It was dissolved in dimethyl sulfoxide (Sigma Aldrich, St. Louis, MO, USA) and stored at −80°C for *in vitro* studies.

Cell Counting Kit-8 assay and IC50 calculation

Cell proliferation in the presence or absence of different concentrations of Adjudin was determined by Cell Counting Kit-8 (CCK-8) assay kit (Yeason, Shanghai, China). Cell suspensions of NCI-H446 (2500 cells) or DMS114 (2×10^4 cells) in a total volume of 100 μL were seeded into individual wells (*n* = 5) of 96-well plates. After treatment, 10 μL CCK-8 solution was added to each well and incubated for one to two hours. The absorbance at 450 nm was measured by the microplate reader (Synergy2; BioTek, Winooski, VT, USA). The IC50 (half maximal inhibitory

concentration) value was calculated by Prism software (GraphPad Software, Inc., La Jolla, CA).

Western blot

Protein levels were detected by western blotting. Cells that were treated differently were lysed with RIPA buffer (Millipore, Temecula, CA, USA) containing protease and phosphatase inhibitor, and PMSF. Protein extracts were quantified by BCA Protein Assay Kit (Pierce, Rockford, IL, USA). After separation by SDS-PAGE, they were then transferred onto 0.45-μm nitrocellulose membranes (Millipore). The membrane was incubated with primary antibodies overnight at 4°C, and then the membrane was hybridized with secondary antibody (1:5000 dilution, Epitomics, China) at room temperature for one hour. The signals were visualized using the ECL system. Antibodies for Western blotting were as follows: SIRT3 (1:1000 dilution, CST); FOXO3a (1:1000, CST); E-cad, N-cad, vimentin (1:1000, CST); GAPDH (1:2000 dilution, Proteintech); and cleaved caspase-3 (1:1000 dilution, CST).

Apoptosis assays

Annexin V-FITC/PI Apoptosis Detection Kit (Lianke, Hangzhou, China) was used to evaluate cell apoptosis after 24 hours in different concentrations of Adjudin. The apoptotic cells with fragmented and condensed nuclei were determined using DAPI staining (Beyotime Biotechnology, Shanghai, China). Finally, photographs were captured under a fluorescence microscope (Leica DMi8, Wetzlar, Germany) equipped with a digital camera.

Cell cycle assays

Cell cycle was determined by flow cytometry. First, 1×10^6 cells were suspended in phosphate-buffered saline and fixed with 70% ethanol. The next day, fixed cells were centrifuged at 1000 *g* for five minutes, washed with ice-cold phosphate-buffered saline and stained with PI/RNase staining buffer (BD, Franklin Lake, NJ, USA) for 15 minutes at room temperature. The DNA contents of cells were analyzed in an FAC Scan flow cytometer (Becton Dickinson, Franklin Lakes, NJ, USA), and the data were analyzed using Modifit software (Verity Software House Company, Tosham, ME, USA).

Transwell assays

NCI-H446 (5×10^4 cells) or DMS114 (5×10^5 cells) with 1% FBS medium were seeded into an 8-μm pore membrane or Matrigel-coated (CORNING, Lowell, MA, USA) membrane Transwell chamber (CORNING, Lowell, MA, USA) placed in a 24-well plate. After cell attachment, 10%
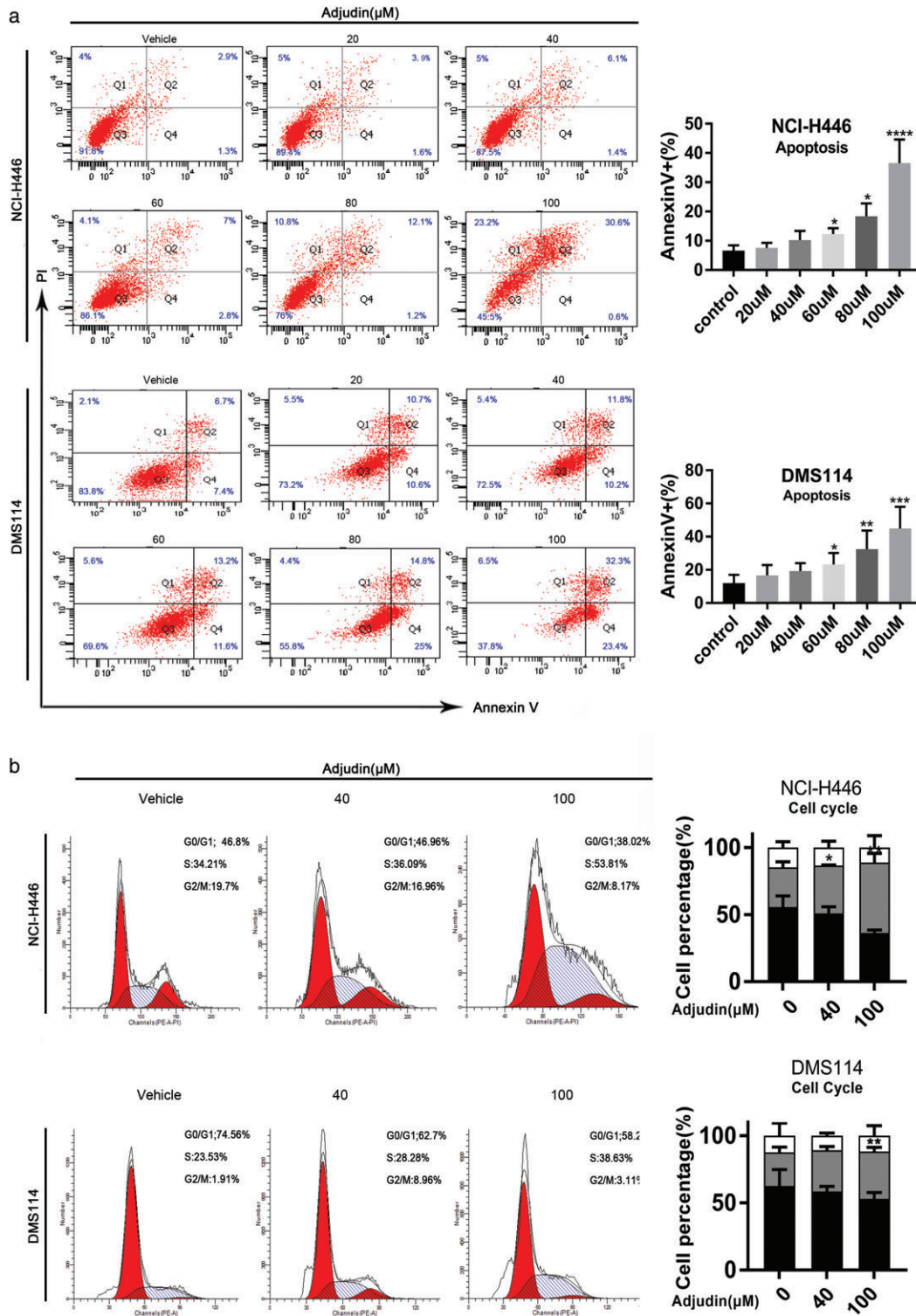
Figure 2 Adjudin induced apoptosis and S cell cycle arrest in small-cell lung cancer cell lines. (**a**) Cells were treated with increased concentrations of Adjudin for 24 hours, and then apoptosis was detected using the Annexin V-FITC/PI Apoptosis Detection Kit as detailed. The LL quadrant (Annexin V–/PI–), LR quadrant (Annexin V+/PI–), and UR quadrant (Annexin V+/PI+) of the histograms indicated the percentage of normal cells, early apoptosis, and late apoptosis, respectively. Data are expressed as a percentage of total cells. (**b**) Cells were treated with the indicated concentrations of Adjudin for 24 hours, and the cell cycle distribution was analyzed by flow cytometry (☐) G2/M, (▦) S, and (■) G0/G1. Values are presented as the mean ± SD, *n* = 3; one-way ANOVA test: *$P < 0.05$, **$P < 0.01$ compared with the control; scale bar, 100 μm.
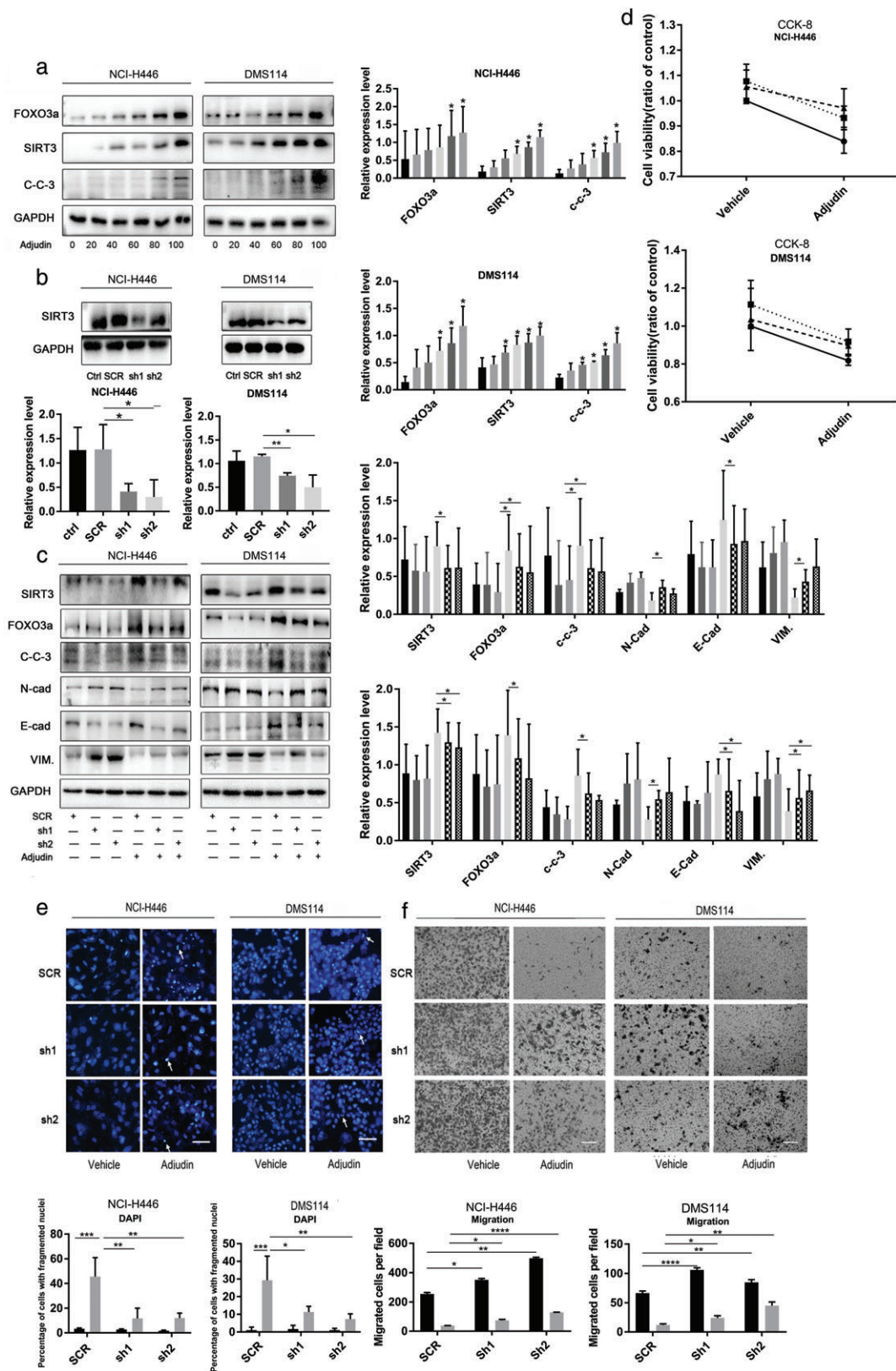
Figure 3 Legend on next page.

FBS medium with Adjudin (40 μM) was added to the lower chamber of the 24-well plate. After 24 hours, migrated or invaded cells were stained. They were photographed, and three microscopic fields were counted.

Scratch assays

Confluent monolayer cells in six-well plates were scratched and cultured with RPMI 1640 medium containing 1% FBS with or without Adjudin. Photomicrographs were taken at 0 and 24 hours after scratching. The scratch healing ratio was calculated as follows: (width of 0 hour − width of 24 hours) / width of 0 hour. Data were analyzed using ImageJ software (National Institutes of Health, Bethesda, MD, USA).

RNA interference and plasmid transfection

Specific short-interfering RNAs targeting Foxo3a (si-foxo3a) and negative control scrambled siRNAs (siRNA-NC) were purchased from HanBio (Shanghai, China). siRNA sequences were as follows: hsFOXO3a-siRNA (5′-CGUGAUGCUUCGCAAUGAU-3′ and 5′-AUCAUUG CGAAGCAUCACG-3′). Plasmid SIRT3-Flag was from Addgene (The nonprofit plasmid repository, www.addgene.org). The cDNA of SIRT3 was cloned into the pLVX-Neo-IRES lentiviral vector (Biowit Company, www.biowit.com.cn). The specific target sequences of SIRT3 (sh1: 5′-CAACGT-CACTCACTACTTT-3′; sh2: 5′-GGGTGCTTCAAGTGT-TGTT-3′) were cloned into the GV298 lentiviral shRNA vector. siRNAs and plasmids were transfected into NCI-H446 and DMS114 cells by Lipofectamine 3000 with or without P3000 (Thermo Company, Waltham, MA, USA) following the manufacturer's instructions. Cells were replaced with fresh medium four to six hours later, and cultured for 48 hours to carry out further experiments.

Analysis of public datasets from GEO, TCGA, and Kaplan–Meier Plotter

Relative mRNA values of SIRT3 and FOXO3a were analyzed from the GEO database. Relative copy number and mRNA levels of SIRT3 and FOXO3a of TCGA were from cBioPortal. Linear regression and Spearman correlations between mRNA levels were conducted. Prognostic values of SIRT3 or FOXO3a mRNA levels were analyzed by Kaplan–Meier survival curves of lung cancer patients using Kaplan–Meier Plotter. The log–rank test was used for statistical analysis.

Animal studies

Five-week old NOD scid gamma mice were maintained in 12-hour light/12-hour dark cycles. Cell suspensions of NCI-H446 (4×10^6 cells) in a volume of 100 μL (phosphate-buffered saline: Matrigel = 4:1) were injected subcutaneously into the right flanks of BALB/c nude mice with insulin injection syringes (BD). Tumors were measured by a caliper every two days. When tumors reached 6–7 mm diameter, the mice were randomly divided into different groups that received both vehicles, and treatment groups that received either Adjudin alone (75 mg/kg/2 days), paclitaxel alone (7.5 mg/kg/3 days), or a combination of Adjudin and paclitaxel ($n = 5$ per group) by intraperitoneal injection. After two weeks of treatment, tumors were collected and photographed, followed by hematoxylin–eosin staining. T/C% was calculated according to the following formula: ($\triangle$treated tumor volume / $\triangle$control tumor volume) × 100%, $\triangle$treated tumor volume means the average tumor volume at the end of the experiment minus the average tumor volume at the beginning of the treatment.[22] All animal experiments were carried out in full accordance with the protocols approved by Institutional Ethics Committee of Shanghai Jiao Tong University.

Figure 3 Knockdown of sirtuin 3 (SIRT3) partially restored the anticancer effect of Adjudin on small-cell lung cancer. (a–c) Cells were treated with Adjudin as mentioned in Fig 1a. Then, the expression of sirtuin 3 (SIRT3) and Forkhead box O3a (FOXO3a) was assessed by western blotting. (**a**) GAPDH was used as a loading control NCI-H446 (——) 0 μM, (——) 20 μM, (——) 40 μM, ( ) 60 μM, (——) 80 μM, and (——) 100 μM, and DMS114 (——) 0 μM, (——) 20 μM, (——) 40 μM, ( ) 60 μM, (——) 80 μM, and (——) 100 μM. (**b**) The knockdown effect of SIRT3 silencing plasmid was determined by western blotting. NCI-H446 and DMS114 cells were transfected with vehicle or SIRT3 silencing shRNA with Lipofectamine 3000 reagent for 24 hours, and then cells were exposed to Adjudin for another 24 hours, western blot analysis of cleaved-caspase-3 (c-c-3) (Adjudin: 60 μM) and EMT-related protein (E-cadherin, N-cadherin, and vimentin) levels (Adjudin 40 μM) (**c**) Vehicle (■) SCR, (■) sh1, and (■) sh2 and Adjudin (☐) SCR, (▦) sh1, and (▦) sh2. (**d**) Cells were treated as described in Fig 3c (Adjudin: 60 μM). Afterwards, cell proliferation was detected using Cell Counting Kit-8 assays NCI-H466 (—●—) SCR, (--■--) sh1, and (--▲--) sh2 and DMS114 (—●—) SCR, (--■--) sh1, and (--▲--) sh2. (**e**) Apoptotic cells were assessed by nuclear fragmentation and condensation (arrows) using DAPI staining. Scale bar, 100 μm. Cells were treated similarly as in Fig 3c (■) vehicle, and (☐) Adjudin. (f) Transwell assays were used to access cell migration. Cells were treated similarly as in Fig 3c, with Adjudin (40 μM) (■) vehicle, and (☐) Adjudin. Data were representative of three independent experiments. Values are presented as the mean ± SD, $n = 3$; one-way ANOVA test: *$P < 0.05$; **$P < 0.01$; ***$P < 0.001$; ****$P < 0.0001$; scale bar, 100 μm.
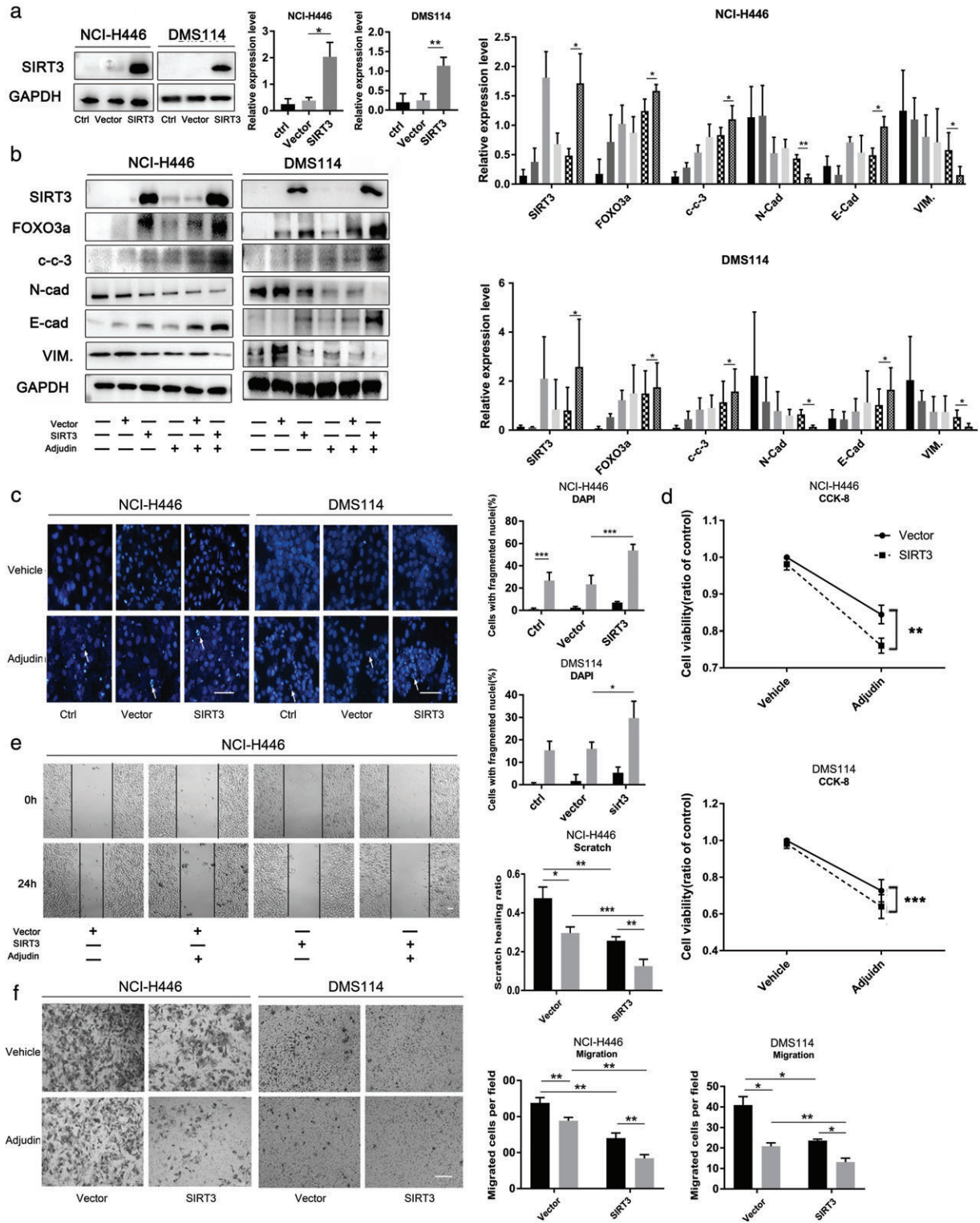
Figure 4 Legend on next page.

Statistical analysis

All data were analyzed using Prism software. They were presented as the means ± SD, and statistical analysis was performed using Student's *t*-tests or ANOVA with Tukey's post-hoc test. *P* < 0.05 was considered statistically significant.

Results

Adjudin showed good anticancer activity in human SCLC cell lines.

The viability of NCI-H446 and DMS114 cells after treatment with Adjudin (Fig 1a) at different concentrations was detected by CCK-8 assay kit. As shown in Figure 1b, Adjudin decreased the viability of NCI-H446 cells in a dose- and time-dependent manner with a maximal dose of 100 μM. Similar results were observed in DMS114 cells. Meanwhile, scratch and Transwell assays showed that Adjudin (40 μM) significantly inhibited cell migration and invasion (Fig 1c,d). Furthermore, the epithelial marker, E-cadherin, was upregulated, and the mesenchymal markers, N-cadherin and vimentin, were downregulated in cells treated with Adjudin (40 μM) for 24 hours (Fig 1e). These results showed that Adjudin significantly inhibits SCLC *in vitro*.

Adjudin induced apoptosis and S cell cycle arrest in SCLC cell lines

We investigated the effects of Adjudin on cell apoptosis and cell cycle by Annexin V-FITC/PI and PI/RNase staining, respectively. The results revealed that the proportion of early and late apoptotic NCI-H446 cells increased 7.43-fold after treatment with 100 μM Adjudin for 24 hours compared with the control, and fourfold in DMS114 cells (Fig 2a). After incubation for 24 hours, 100 μM Adjudin increased the number of NCI-H447 cells in the S phase by 19.6% compared with the control, and 15.1% in DMS114 cells (Fig 2b). Based on these data,

Adjudin suppressed cell proliferation by regulating cell cycle and apoptosis.

Knockdown of SIRT3 partially restored the anticancer effect of Adjudin on SCLC

We further explored the modulatory mechanism by which Adjudin functions. We showed that Adjudin upregulated protein expression of SIRT3, FOXO3a, and cleaved-caspase-3 in a dose-dependent manner in SCLC cells (Fig 3a) compared with the control. We next examined whether the Adjudin-induced anticancer effect was related to SIRT3 and FOXO3a. Silencing SIRT3 by plasmid significantly reduced protein expression of SIRT3 and FOXO3a (Fig 3b,c), which significantly reversed the Adjudin-induced cell growth, migration inhibition and apoptosis promotion (Fig 3d–f). EMT-related markers and cleaved caspase-3 also changed accordingly. Downregulation of SIRT3 decreased the expression of E-cadherin and cleaved caspase-3, but the inhibition was reduced after cells were exposed to Adjudin. The expression of N-cadherin and vimentin was higher after transfection with silencing SIRT3 plasmid, and the promotion was restored after Adjudin treatment (Fig 3c). The above results demonstrated that downregulating SIRT3 could attenuate Adjudin-induced SCLC cells inhibition.

Overexpression of SIRT3 enhanced the efficacy of Adjudin in SCLC cells

We further tested the potential functions of SIRT3, exploring whether SIRT3 could strengthen the effect of Adjudin on SCLC cells. Cells were transfected with SIRT3 overexpression plasmid or negative control plasmid (Fig 4a,b). The apoptosis rate was upregulated when SIRT3 was overexpressed, and that increase was more pronounced with Adjudin treatment (Fig 4c), as shown by DAPI staining. The protein level of cleaved caspase-3 changed similarly (Fig 4b). Cell proliferation (Fig 4d) and migration (Fig 4e,f) were suppressed after transfection with SIRT3 overexpression plasmid; SIRT3 overexpression also decreased the expression of N-cadherin and vimentin, and increased the expression of E-cadherin (Fig 4b). Furthermore, the overexpression of

Figure 4 Overexpression of sirtuin 3 (SIRT3) enhanced the efficacy of Adjudin in small-cell lung cancer cells. (**a**) Western blot analysis of SIRT3 and Forkhead box O3a (FOXO3a) in vector and SIRT3-overexpressed transfected cells. After transfection for 24 hours, cells were treated with Adjudin (60 μM) for another 24 hours. (**b**) Western blot analysis of SIRT3, FOXO3A, cleaved caspase-3 and EMT-related marker (E-cadherin, N-cadherin and vimentin) levels vehicle (■) ctrl, (■) vector, and (■) SIRT3, and Adjudin (▢) ctrl, (▨) Vector, and (▨) SIRT3. (**c**) Apoptotic cells were assessed by nuclear fragmentation and condensation (arrows) using DAPI staining. Cells were treated as described in (**b**) NCI-H446 (■) vehicle, and (▢) Adjudin and DMS114 (■) vehicle, and (▢) Adjudin. (**d**) Cell proliferation was detected using Cell Counting Kit-8 assays. Cells were treated as described in B NCI-H446 (—●—) vector, and (--■--) SIRT3 and DMS114 (—●—) vector, and (--■--) SIRT3. (**e**) Scratch NCI-H446 (■) vehicle, and (▢) Adjudin and (**f**) Transwell assays were used to evaluate cell migration NCI-H446 (■) vehicle, and (▢) Adjudin and DMS114 (■) vehicle, and (▢) Adjudin. Cells were treated similarly as in Fig 4b, with Adjudin (40 μM). Values are presented as the mean ± SD, *n* = 3; one-way ANOVA test: *P < 0.05; **P < 0.01; ***P < 0.001; ****P < 0.0001; scale bar, 100 μm.
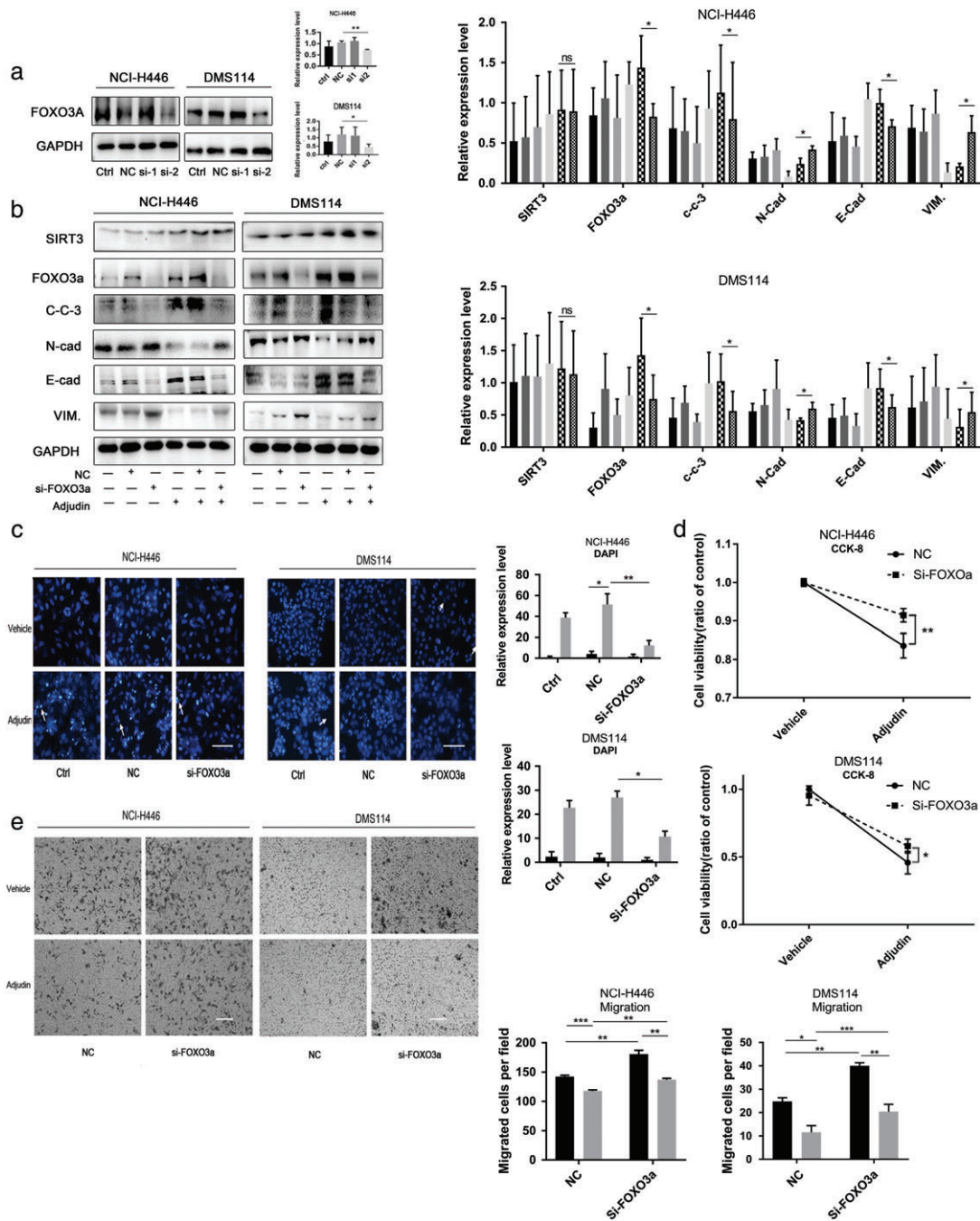
Figure 5 Downregulation of Forkhead box O3a (FOXO3a) also reduced the efficacy of Adjudin. (**a**) The knockdown effect of FOXO3a siRNA was determined by western blot. (**b**) NCI-H446 and DMS114 were transfected with control or FOXO3a siRNA with Lipofectamine 3000 reagent for 24 hours; then, cells were exposed to Adjudin (60 or 40 μM) for another 24 hours. Western blot analysis of EMT-related protein (E-cadherin, N-cadherin, and vimentin) and cleaved caspase-3 levels vehicle (■) ctrl, (▨) NC, and (▨) Si-FOXO3a and Adjudin (☐) ctrl, (▨) NC, and (▨) Si-FOXO3a. (c) Apoptotic cells were assessed by nuclear fragmentation and condensation (arrows) using DAPI staining. (d) Cells were treated as described in Fig 5b. Afterwards, the cell proliferation was detected using Cell Counting Kit-8 assays NCI-H446 (—●—) NC, and (--■--) Si-FOXOa and DMS114 (—●—) NC, and (--■--) Si-FOXOa. (e) Transwell assays were used to evaluate cell migration after being treated as described. Cells were treated similarly as in Fig 5b, with Adjudin (40 μM) NCI-H446 (■) vehicle, and (☐) Adjudin and DMS114 (■) vehicle, and (☐) Adjudin. Values are presented as the mean ± SD, *n* = 3; *$P < 0.05$; **$P < 0.01$; ***$P < 0.001$; ****$P < 0.0001$; scale bar, 100 μm.

Figure 6 Adjudin upregulated Forkhead box O3a (FOXO3a) by activating sirtuin 3 (SIRT3). (**a**) Western blot analysis of SIRT3, FOXO3A, cleaved caspase-3, and EMT-related proteins. NCI-H446 cells were transfected with FOXO3A siRNA or NC siRNA in SIRT3-overexpressing NCI-H446 cells. After 24 hours, cells were treated with Adjudin (60 μM) for an additional 24 hours. Then, cell lysates were harvested (▥) SIRT3+NC, (▨) SIRT3+NC, (▭) SIRT3+si-FOXO3a, and (▧) SIRT3+si-FOXO3a. (**b**) Apoptotic cells were assessed by nuclear fragmentation and condensation (arrows) using DAPI staining. Scale bar, 100 μm. Cells were treated as described in Fig 6a (■) Vehicle, and (□) Adjudin. (**c**) Cell proliferation was detected using Cell Counting Kit-8 assays. They were treated as described in (**a**) (—●—) SIRT3+NC, and (--■--) SIRT3+si-FOXO3a. (**d**) Transwell assays were used to access cell migration. Cells were treated similarly as in Fig 6a, with Adjudin (40 μM) (■) vehicle, and (□) Adjudin. Values are presented as the mean ± SD, n = 3; one-way ANOVA test: *$P < 0.05$; **$P < 0.01$; ***$P < 0.001$; ****$P < 0.0001$; scale bar, 100 μm.
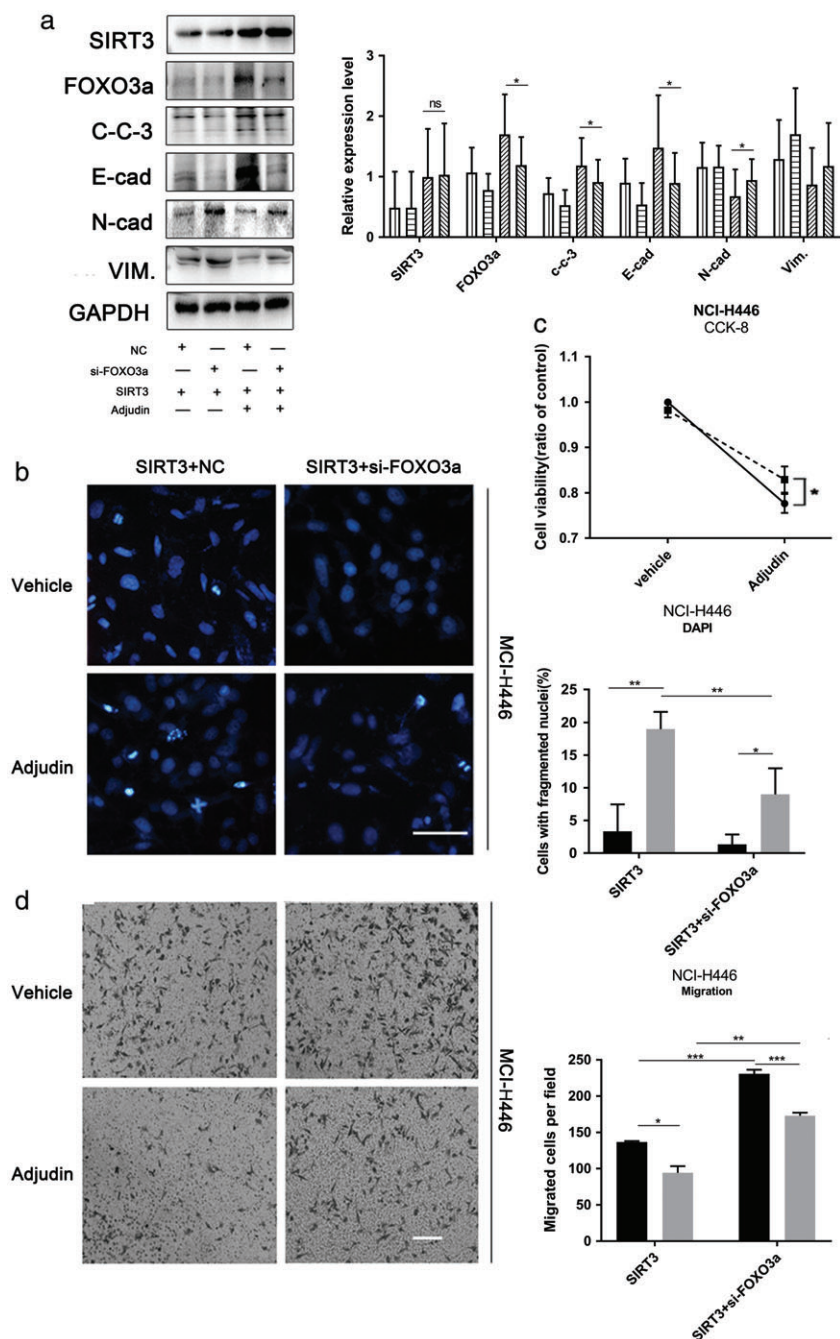
SIRT3 upregulated the protein level of FOXO3a (Fig 4b). Collectively, these results confirmed that overexpression of SIRT3 enhanced the effect of Adjudin in SCLC cells.

Downregulation of FOXO3a reduced the efficacy of Adjudin

In our further study, we found that silencing of FOXO3a by siRNA (silencing effects were tested by western blotting, shown in Fig. 5a) significantly reversed the Adjudin-induced anti-

SCLC effect (Fig 5c–e). Silencing of FOXO3a never influenced the expression of SIRT3 (Fig 5b), with or without Adjudin.

Taken together, these results suggested that SIRT3 and FOXO3a both play positive roles in Adjudin-induced growth and migration inhibition in SCLC cells.

Adjudin upregulated FOXO3a by activating SIRT3

Previously, it was reported that the SIRT3–FOXO3a signaling pathway was involved in the inhibitory effect of
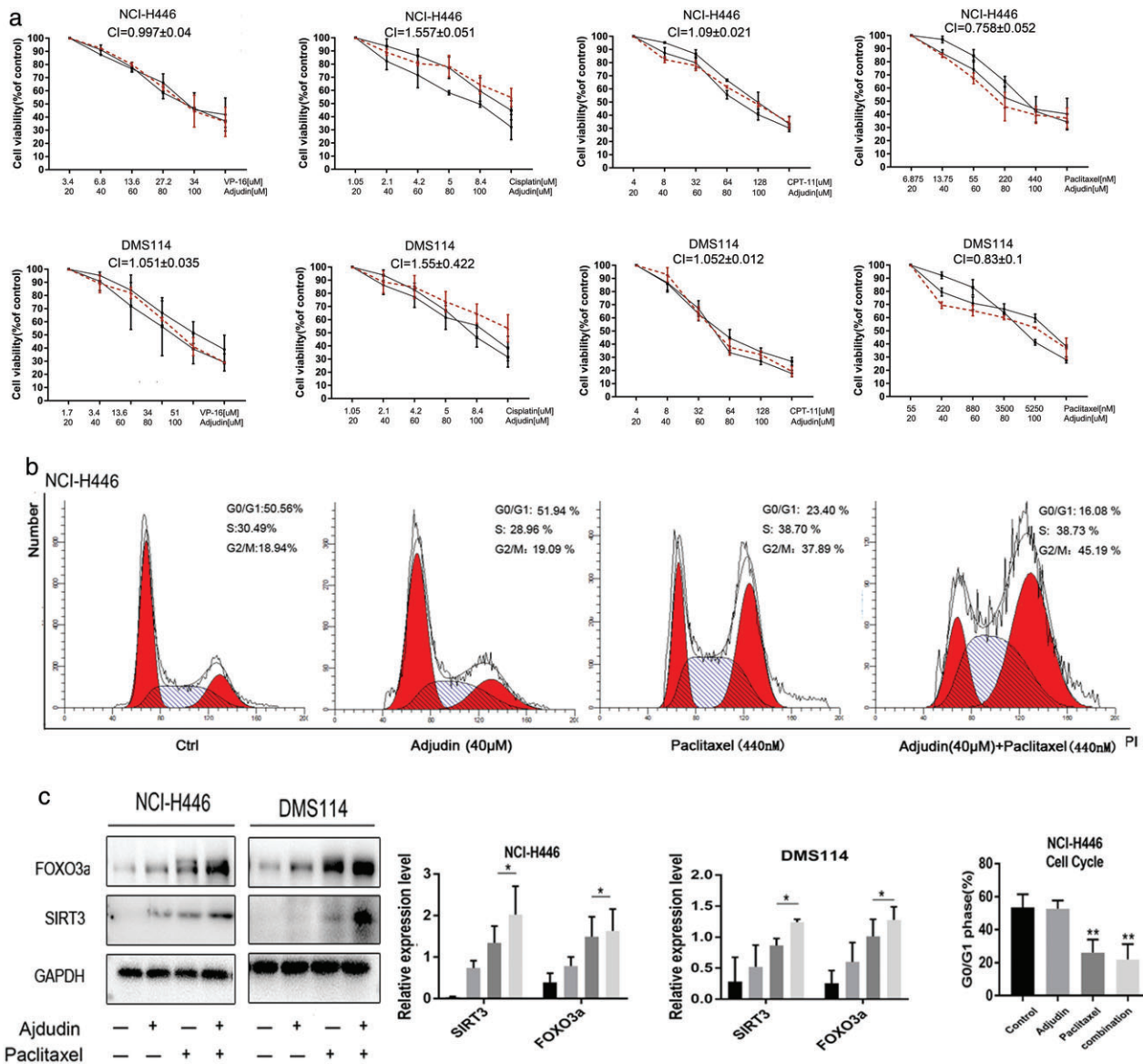
Figure 7 Adjudin synergized with paclitaxel *in vitro*. (**a**) The proliferation of NCI-H446 and DMS114 cells was detected using Cell Counting Kit-8 viability assays when Adjudin was combined with cisplatin, etoposide, irinotecan, or paclitaxel in a ratio of 1:1 after 48 hours as indicated (see Methods). The results reveal synergy with paclitaxel (combination indexes [CI] average 0.756) (—●—) paclitaxel, (—◆—) Adjudin, and (--■--) combination (1:1), antagonism with cisplatin (CI average 1.557) (—●—) cisplatin, (—◆—) Adjudin, and (--■--) combination (1:1), and addition with etoposide and irinotecan (CI 0.997and 1.09, respectively) (—●—) etoposide, (—◆—) Adjudin, and (--■--) combination (1:1) and (—●—) irinotecan, (—◆—) Adjudin, and (--■--) combination (1:1) in NCI-H446. (**b**) Cell cycle analysis of NCI-H446 cells treated with Adjudin (40 μM), paclitaxel (440 nM), and the combination after 24 hours. (**c**) The protein levels of sirtuin 3 (SIRT3) and Forkhead box O3a (FOXO3a) were analyzed by western blotting NCI-H446 (——) ctrl, (——) Adjudin, (——) paclitaxel, and (——) combination (1:1) and DMS114 (——) ctrl, (——) Adjudin, (——) paclitaxel, and (——) combination (1:1). Cells were treated as described in Fig 7b. Values are presented as the mean ± SD, $n = 3$; one-way ANOVA test: *$P < 0.05$; **$P < 0.01$; ***$P < 0.001$; ****$P < 0.0001$; scale bar, 100 μm.

Adjudin on astrocyte activation.[15] Therefore, we hypothesized that this pathway also played a significant role in the anticancer effect of Adjudin on SCLC cells. In our study, FOXO3a siRNA was used to transfect cells that had already overexpressed SIRT3. The expression of FOXO3a was downregulated after transfection, with or without Adjudin treatment (Fig 6a). The results showed that the increased apoptosis rate (Fig 6b), decreased proliferation (Fig 6c), and migrated cells (Fig 6d) were apparently reversed. In conclusion, Adjudin upregulated FOXO3a by activating SIRT3.
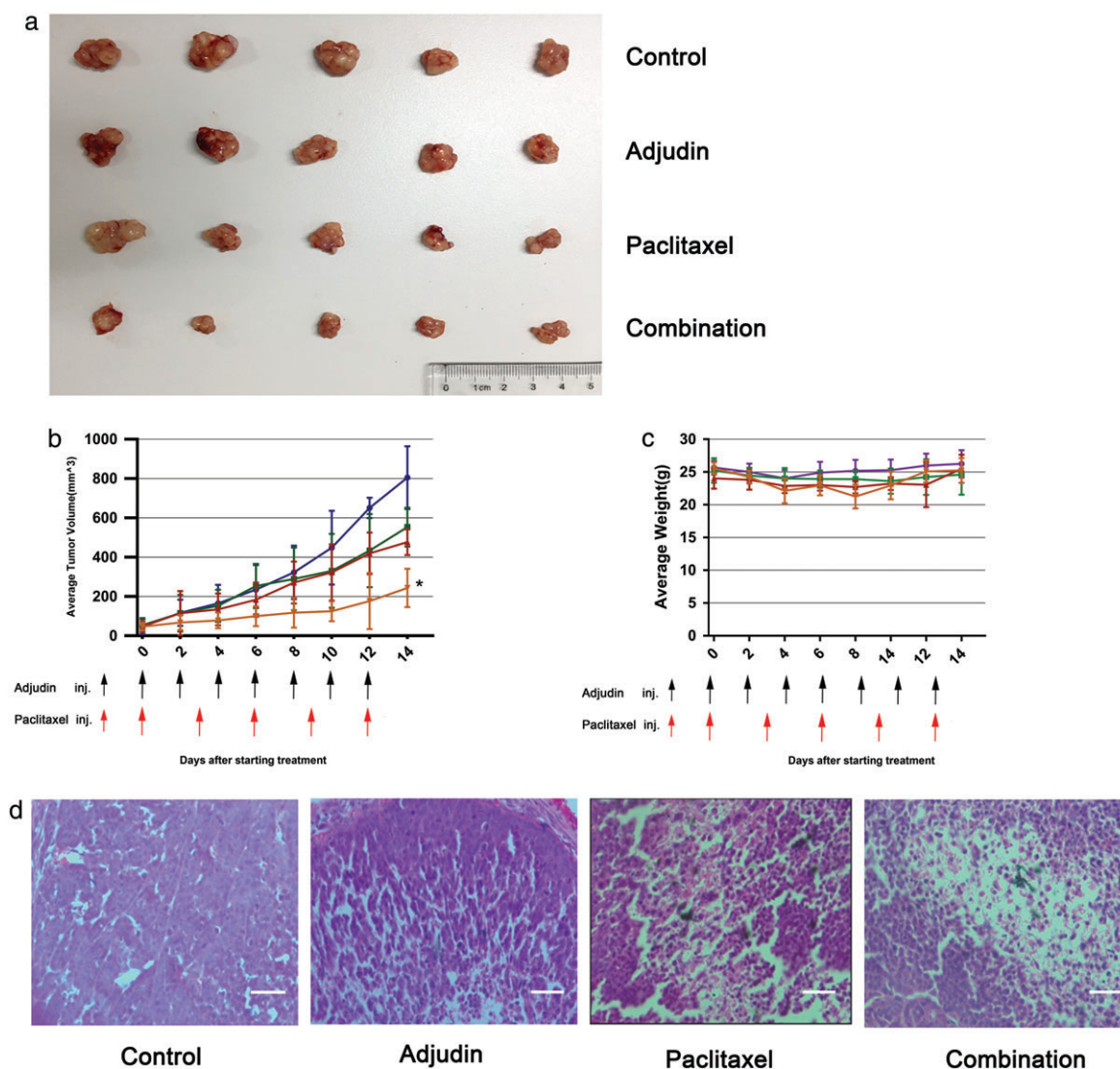
Figure 8 Synergistic effect of Adjudin and paclitaxel *in vivo.* (**a**) Cell suspensions of NCI-H446 (4×10^6 cells) in a volume of 100 μL were injected subcutaneously into the right flanks of BALB/c nude mice. When tumors reached 6–7 mm in diameter, the mice were randomly divided into four different groups as described. Imaging of subcutaneous tumor nodules from each group. The tumors were excised after two weeks of treatment. (**b**) The curves of tumor volumes in different groups are shown in the line chart, during two weeks of treatment (—●—) vehicle, (—■—) Adjudin, (—▲—) paclitaxel, and (—▼—) combination. (**c**) Mouse weights in each group were calculated every two days, according to the detection of each mouse. (**d**) Hematoxylin–eosin staining of all the tumors of subcutaneous lung cancer xenograft models was performed (—●—) vehicle, (—■—) Adjudin, (—▲—) paclitaxel, and (—▼—) combination. Scale bar, 100 μm. Values are presented as the mean ± SD, $n = 3$; one-way ANOVA test: *$P < 0.05$; **$P < 0.01$.

Adjudin synergized with paclitaxel *in vitro*

Having established that Adjudin can effectively inhibit cell proliferation, we sought to determine if Adjudin would synergize with chemotherapeutic drugs commonly used in SCLC treatment. We examined the concomitant combination of Adjudin with four chemotherapeutic drugs in a 1:1 ratio (Fig 7a): etoposide, cisplatin, irinotecan, and paclitaxel, which are clinically used in SCLC. CCK-8 assays were performed to analyze the combination activity. Combination concentrations of individual compounds were

adjusted based on their IC50 in the cells. The average combination indexes (CI)[23] of the 50% growth inhibition were calculated for each combination. It is possible to classify the combination effect, based on the CI value, as synergistic, additive, or antagonistic. In NCI-H446 cells, our results revealed that there was antagonism between Adjudin and cisplatin (CI average: 1.557). Adjudin weakly synergized with paclitaxel (CI average: 0.756). Adjudin combined with etoposide (CI average: 0.997) or irinotecan (CI average: 1.090) may only achieve additivity. Similar results were

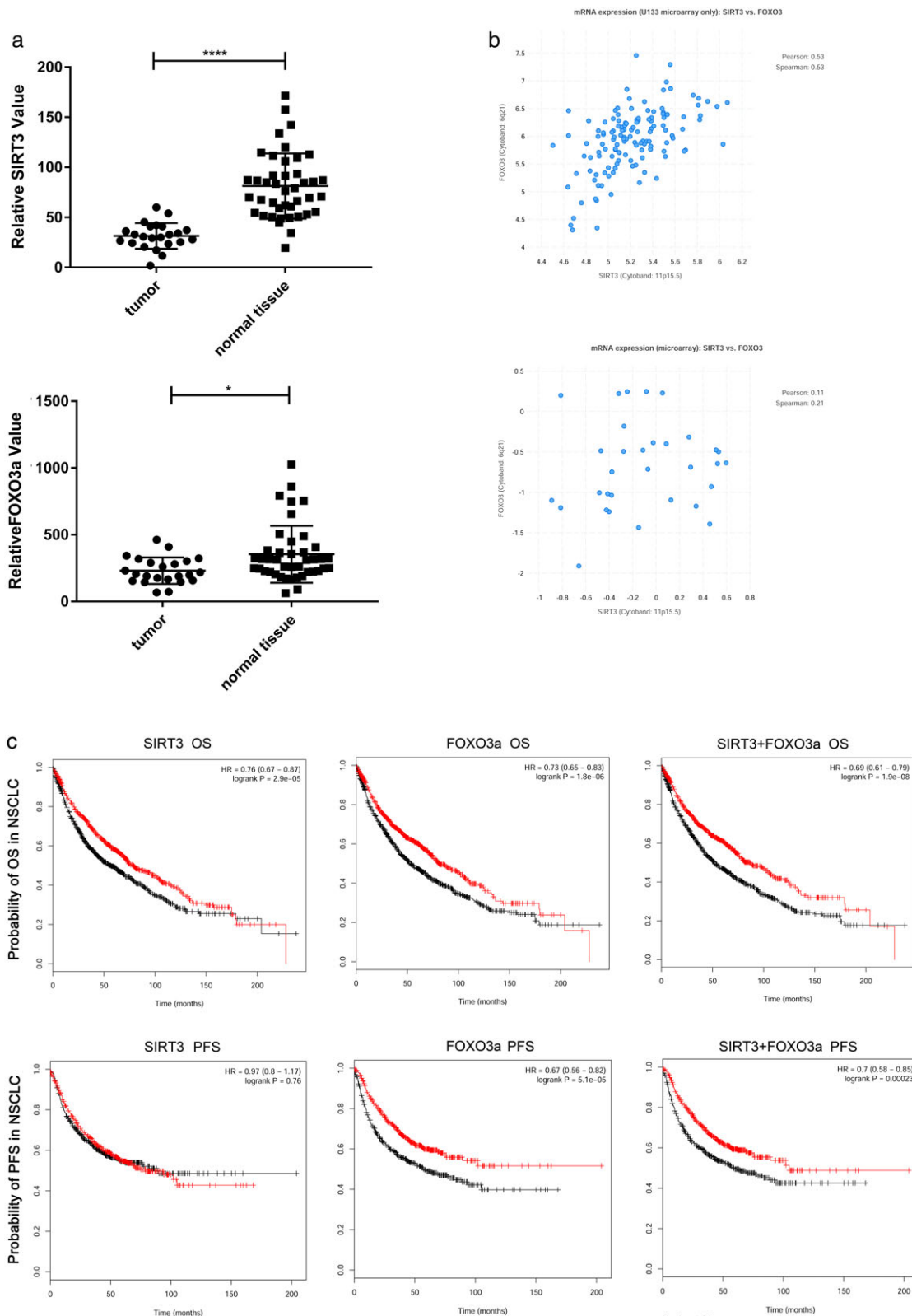**Figure 9** Legend on next page.

observed in DMS114 cells (Fig 7a; CI <0.9 indicated synergy, $0.9 \leq CI \leq 1.1$ indicated additivity, and CI >1.1 indicated antagonism). The influence of the combination use of Adjudin and paclitaxel on the cell cycle is demonstrated in Figure 7b. Obviously, proportions of cells in the S and M phase were significantly increased in the combination group. In addition, combination treatment upregulated the protein expression of SIRT3 and FOXO3a (Fig 7c).

Synergistic effect of Adjudin and paclitaxel *in vivo*

After subcutaneous lung cancer mouse models were established with NCI-H446 cells, they were randomly assigned to four groups: Adjudin (75 mg/kg/2 days), paclitaxel (7.5 mg/kg/3 days), combination (Adjudin 75 mg/kg/2 days, paclitaxel 7.5 mg/kg/3 days), or vehicle as control (Fig 8). The tumor was measured by a caliper every two days, and tumor volume is demonstrated in Figure 8a,b. Obviously, tumor growth was markedly suppressed in the combination group, compared with the vehicle group, with a T/C% value of 21.47%. By contrast, the T/C% values of the remaining groups were 66.859% (Adjudin) and 58.89% (paclitaxel), respectively. The T/C value represents relative changes of the average tumor volumes in drug-treated groups compared with the control group.[22] Hematoxylin–eosin staining of tumors revealed that combination treatment of Adjudin and paclitaxel decreased tumor density (Fig 8d). All those data revealed that Adjudin had a synergistic effect with paclitaxel *in vivo*.

Prognostic and diagnostic values of SIRT3 and FOXO3a in lung cancer patients according to databases

To test the prognostic and diagnostic values of SIRT3 and FOXO3a in lung cancer, we tried to find clues from the databases. First, we explored microarray datasets in the GEO database. As shown in Figure 9a, the values of SIRT3 and FOXO3a significantly decreased in SCLC tumors compared with normal tissues (65 samples in total, 23 samples were SCLC tumors, and 42 samples were normal tissues). Next, we analyzed the mRNA expression of SIRT3 and FOXO3a in NSCLC in the TCGA database in 133 lung squamous cell carcinoma and 32 lung adenocarcinoma carcinoma samples; a positive correlation between expression of SIRT3 and FOXO3a was observed in both

(Fig 9b) subtypes. Finally, higher mRNA levels of SIRT3, FOXO3a or total were associated with longer overall survival and progression-free survival (Fig 9c). Therefore, they might be potential biomarkers to evaluate the diagnosis of lung cancer patients. In conclusion, our findings revealed that SCLC patients have lower expression of SIRT3 and FOXO3a; these proteins are positively related and are associated with good prognosis in lung cancer patients.

Discussion

The present results showed that Adjudin inhibited SCLC cell growth and migration. We first reported that the SIRT3-FOXO3a signaling pathway mediated the inhibitory effect of Adjudin against SCLC, and SIRT3 and FOXO3a levels might be good predictors of patients' prognosis in lung cancer. Furthermore, we also showed that Adjudin and paclitaxel are synergistic *in vitro* and *in vivo*. Surgical resection, chemotherapy, targeted therapy, and immunotherapy have acquired brilliant success in NSCLC.[24] Small molecule cytotoxic drugs rarely have broad applications and bright prospects. However, for SCLC patients, many NSCLC-effective drugs are not effective, and furthermore, few patients can undergo surgery.[25] Therefore, Adjudin is a crucial discovery for SCLC. Paclitaxel belongs to the class of diterpenoid compounds (mitotic inhibitors) derived from *Taxus brevifolia* that exert efficient, broad-spectrum chemotherapeutic effects against various cancer types.[26–28] Paclitaxel can arrest cells in the M phase, and is one of the most widely used drugs in SCLC. However, it can cause a few side-effects, including hair loss, allergic reactions, and so on. Other serious side-effects include arrhythmia, bone marrow suppression, and lung inflammation. We confirmed that Adjudin was synergetic with paclitaxel, which decreased the dosage of paclitaxel and reduced side-effects. Adjudin had additivity effects with VP-16 or CPT-11 (the two most commonly used chemotherapy drugs in SCLC) as well. These results suggest that Adjudin could be a potential adjuvant for chemotherapy. With the development of new treatments for cancers, Adjudin might yield better efficacy in the future. We are trying to investigate its potential in this area.

The mechanism of the synergetic combination effect is unknown. Here are several conjectures: (i) the combination significantly inhibited mitosis (results of flow cytometry

Figure 9 The prognostic and diagnostic values of sirtuin 3 (SIRT3) and Forkhead box O3a (FOXO3a) in lung cancer patients according to databases. (**a**) SIRT3 and FOXO3a levels in small cell lung cancer tumor and normal tissues from the GEO database (65 samples in total; 23 samples were small cell lung cancer tumors, and 42 samples were normal tissues; Student's *t*-test, *$P < 0.05$, ****$P < 0.001$). (**b**) Linear regression and Pearson correlation of mRNA levels between SIRT3 and FOXO3a in lung squamous cell carcinoma (133 samples) and lung adenocarcinoma carcinoma (32 samples) patients from the TCGA database. (**c**) Relationship between SIRT3, FOXO3a, or total mRNA level with overall survival (OS) and progression-free survival (PFS) in non-small cell lung cancer (NSCLC), evaluated by Kaplan–Meier Plotter. Statistical analysis was performed using the log–rank test expression (——) low, and (——) high.

analysis showed that combination group caused higher arrest rates in the S and M phases, leading to a considerable increase in apoptosis and necrosis); (ii) previous studies reported that Adjudin affected cell mitochondrial function and energy metabolism,[2] thus after Adjudin treatment, cells became more vulnerable to paclitaxel; and (iii) upregulation of FOXO3a enhances the cytotoxicity of paclitaxel in breast cancer,[29–31] and FOXO3a is critical for E1A gene-mediated chemosensitization to paclitaxel in cancer cells.[31] As shown in the present study, the combination usage significantly increased the expression level of FOXO3a.

Many lines of evidence have demonstrated a connection between sirtuins and carcinogenesis. The seven sirtuins are potential prognostic and diagnostic biomarkers for cancers.[32] SIRT1 and SIRT7 function as oncogenes.[33] Others are tumor suppressors.[34] SIRT3 has been regarded as a tumor suppressor by protecting cells from reactive oxygen species accumulation, promoting oxidative phosphorylation to generate adenosine triphosphate, and regulating hypoxia inducible factor-1α.[32,35,36] However, in head and neck squamous cell carcinoma, where SIRT3 is overexpressed, SIRT3 can maintain reactive oxygen species levels at the appropriate levels, and prevent apoptosis and promote carcinogenesis.[37] Here, we further confirmed that SIRT3 functions as a tumor suppressor in SCLC cells. Upregulation of SIRT3 enhances the antitumor effect of Adjudin. In conclusion, Adjudin targeting SIRT3 provides us with new targets for cancer therapy.

FOXO3a also has a double-sided role. It functions as an oncogene in triple-negative breast cancer,[38] acute myeloid leukemia patients[39] and so on. However, in uveal,[40] breast, and prostate cancers,[41] researchers found it was a suppressor gene. Research on FOXO3a has not yet been conducted in SCLC. According to the present study, FOXO3a can function as a tumor suppressor in SCLC. The effects of Adjudin, an effective FOXO3a activator, were partially abrogated by FOXO3a silencing in SCLC.

Previous evidence showed that the SIRT3–FOXO3a axis was a tumor suppressor in many cancers[42–44] it influenced EMT,[45] proliferation[46] and apoptosis.[47] Here, we confirmed that Adjudin activated the SIRT3–FOXO3a axis in SCLC, and the anticancer effect of Adjudin can be influenced by the expression levels of SIRT3 and FOXO3a. More importantly, the relative mRNA levels of FOXO3a and SIRT3 were lower in SCLC than in normal tissues, according to the GEO database. People with higher SIRT3 and FOXO3a had better prognosis (longer overall survival and progression-free survival). The mechanism by which SIRT3 upregulated FOXO3a is not clear. Studies have shown that the Wnt

signaling pathway is associated with it.[45,48] Further research is required.

In conclusion, the present study demonstrates that Adjudin is effective in SCLC cells, and synergizes well with paclitaxel both *in vivo* and *in vitro*, potentially due to Adjudin's effects on the SIRT3–FOXO3a axis. It is a widely studied signaling pathway whose roles vary in different cancers. Database studies have confirmed that the levels of SIRT3 and FOXO3a are closely related in NSCLC, and they are also related to the prognosis of lung cancer patients. Taken together, these results reveal that Adjudin may be available in the treatment of SCLC in the future (especially in combination with other agents), and that SIRT3 and FOXO3a levels may be good predictors of patients' prognosis in lung cancer.

Acknowledgments

Disclosure

No authors report any conflict of interest.

References

1 Hong QY, Wu GM, Qian GS *et al.* Prevention and management of lung cancer in China. *Cancer* 2015; **121** (Suppl 17): 3080–8.

2 Rudin CM, Poirier JT. Small-cell lung cancer in 2016: Shining light on novel targets and therapies. *Nat Rev Clin Oncol* 2017; **14** (2): 75–6.

3 Alexandrov LB, Ju YS, Haase K *et al.* Mutational signatures associated with tobacco smoking in human cancer. *Science* 2016; **354** (6312): 618–22.

4 Abdel-Rahman O. *Changing epidemiology of elderly small cell lung cancer patients over the last 40 years; a SEER database analysis. Clin Respir J* 2018; **12** (3): p. 1093–1099.

5 Farago AF, Keane FK. Current standards for clinical management of small cell lung cancer. *Transl Lung Cancer Res* 2018; **7** (1): 69–79.

6 Socinski MA, Smit EF, Lorigan P *et al.* Phase III study of pemetrexed plus carboplatin compared with etoposide plus carboplatin in chemotherapy-naive patients with extensive-stage small-cell lung cancer. *J Clin Oncol* 2009; **27** (28): 4787–92.

7 Xia W, Geng K. A sirtuin activator and an anti-inflammatory molecule-multifaceted roles of adjudin and its potential applications for aging-related diseases. *Semin Cell Dev Biol* 2016; **59**: 71–8.

8 Xie QR, Liu Y, Shao J *et al.* Male contraceptive Adjudin is a potential anti-cancer drug. *Biochem Pharmacol* 2013; **85** (3): 345–55.

9 Grima J, Silvestrini B, Cheng CY. Reversible inhibition of spermatogenesis in rats using a new male contraceptive, 1-(2,4-dichlorobenzyl)-indazole-3-carbohydrazide. *Biol Reprod* 2001; **64** (5): 1500–8.

10 Sarkar O, Xia W, Mruk DD. Adjudin-mediated junction restructuring in the seminiferous epithelium leads to displacement of soluble guanylate cyclase from adherens junctions. *J Cell Physiol* 2006; **208** (1): 175–87.

11 Cheng CY, Mruk D, Silvestrini B *et al*. AF-2364 [1-(2,4-dichlorobenzyl)-1H-indazole-3-carbohydrazide] is a potential male contraceptive: A review of recent data. *Contraception* 2005; **72** (4): 251–61.

12 Cheng CY, Silvestrini B, Grima J *et al*. Two new male contraceptives exert their effects by depleting germ cells prematurely from the testis. *Biol Reprod* 2001; **65** (2): 449–61.

13 Mruk DD, Wong CH, Silvestrini B, Cheng CY. A male contraceptive targeting germ cell adhesion. *Nat Med* 2006; **12** (11): 1323–8.

14 Xia W, Wong EWP, Mruk DD, Cheng CY. TGF-beta3 and TNFalpha perturb blood-testis barrier (BTB) dynamics by accelerating the clathrin-mediated endocytosis of integral membrane proteins: A new concept of BTB regulation during spermatogenesis. *Dev Biol* 2009; **327** (1): 48–61.

15 Yang X, Geng K, Zhang J, Zhang Y, Shao J, Xia W. Sirt3 mediates the inhibitory effect of Adjudin on astrocyte activation and glial scar formation following ischemic stroke. *Front Pharmacol* 2017; **8**: 943.

16 Li X, Gao C, Wu Y, Cheng CY, Xia W, Zhang Z. Combination delivery of Adjudin and doxorubicin via integrating drug conjugation and nanocarrier approaches for the treatment of drug-resistant cancer cells. *J Mater Chem B* 2015; **3** (8): 1556–64.

17 Quan Y, Xia L, Shao J *et al*. Adjudin protects rodent cochlear hair cells against gentamicin ototoxicity via the SIRT3-ROS pathway. *Sci Rep* 2015; **5**: 8181.

18 Haigis MC, Deng CX, Finley LWS, Kim HS, Gius D. SIRT3 is a mitochondrial tumor suppressor: A scientific tale that connects aberrant cellular ROS, the Warburg effect, and carcinogenesis. *Cancer Res* 2012; **72** (10): 2468–72.

19 Jeong SM, Lee J, Finley LWS, Schmidt PJ, Fleming MD, Haigis MC. SIRT3 regulates cellular iron metabolism and cancer growth by repressing iron regulatory protein 1. *Oncogene* 2015; **34** (16): 2115–24.

20 Torrens-Mas M, Oliver J, Roca P, Sastre-Serra J. SIRT3: Oncogene and tumor suppressor in cancer. *Cancers (Basel)* 2017; **9** (7): 90.

21 Tran H, Brunet A, Grenier JM *et al*. DNA repair pathway stimulated by the forkhead transcription factor FOXO3a through the Gadd45 protein. *Science* 2002; **296** (5567): 530–4.

22 Lai CH, Park KS, Lee DH *et al*. HSP-90 inhibitor ganetespib is synergistic with doxorubicin in small cell lung cancer. *Oncogene* 2014; **33** (40): 4867–76.

23 Naumova E, Ubezio P, Garofalo A *et al*. The vascular targeting property of paclitaxel is enhanced by SU6668, a receptor tyrosine kinase inhibitor, causing apoptosis of endothelial cells and inhibition of angiogenesis. *Clin Cancer Res* 2006; **12** (6): 1839–49.

24 Herbst RS, Morgensztern D, Boshoff C. The biology and management of non-small cell lung cancer. *Nature* 2018; **553** (7689): 446–54.

25 Gazdar AF, Bunn PA, Minna JD. Small-cell lung cancer: What we know, what we need to know and the path forward. *Nat Rev Cancer* 2017; **17** (12): 725–37.

26 Jeong JY, Kim KS, Moon JS *et al*. Targeted inhibition of phosphatidyl inositol-3-kinase p110beta, but not p110alpha, enhances apoptosis and sensitivity to paclitaxel in chemoresistant ovarian cancers. *Apoptosis* 2013; **18** (4): 509–20.

27 McGuire WP, Rowinsky EK, Rosenshein NB *et al*. Taxol: A unique antineoplastic agent with significant activity in advanced ovarian epithelial neoplasms. *Ann Intern Med* 1989; **111** (4): 273–9.

28 Quispe-Soto ET, Calaf GM. Effect of curcumin and paclitaxel on breast carcinogenesis. *Int J Oncol* 2016; **49** (6): 2569–77.

29 Sunters A, Fernández de Mattos S, Stahl M *et al*. FoxO3a transcriptional regulation of Bim controls apoptosis in paclitaxel-treated breast cancer cell lines. *J Biol Chem* 2003; **278** (50): 49795–805.

30 de Moraes GN, Khongkow P, Gong C *et al*. Forkhead box K2 modulates epirubicin and paclitaxel sensitivity through FOXO3a in breast cancer. *Oncogene* 2015; **4**: e167.

31 Su J-L, Cheng X, Yamaguchi H *et al*. FOXO3a-dependent mechanism of E1A-induced Chemosensitization. *Cancer Res* 2011; **71**: 6878–87.

32 Someya S, Yu W, Hallows WC *et al*. Sirt3 mediates reduction of oxidative damage and prevention of age-related hearing loss under caloric restriction. *Cell* 2010; **143** (5): 802–12.

33 Luo J, Nikolaev AY, Imai SI *et al*. Negative control of p53 by Sir2alpha promotes cell survival under stress. *Cell* 2001; **107** (2): 137–48.

34 Kim HS, Vassilopoulos A, Wang RH *et al*. SIRT2 maintains genome integrity and suppresses tumorigenesis through regulating APC/C activity. *Cancer Cell* 2011; **20** (4): 487–99.

35 Zou X, Zhu Y, Park SH *et al*. SIRT3-mediated dimerization of IDH2 directs cancer cell metabolism and tumor growth. *Cancer Res* 2017; **77** (15): 3990–9.

36 Bell EL, Emerling BM, Ricoult SJH, Guarente L. SirT3 suppresses hypoxia inducible factor 1α and tumor growth by inhibiting mitochondrial ROS production. *Oncogene* 2011; **30**: 2986–96.

37 Lai CC, Lin PM, Lin SF *et al*. Altered expression of SIRT gene family in head and neck squamous cell carcinoma. *Tumour Biol* 2013; **34** (3): 1847–54.

38 Rehman A, Kim Y, Kim H *et al*. FOXO3a expression is associated with lymph node metastasis and poor disease-free survival in triple-negative breast cancer. *J Clin Pathol* 2018; **71** (9): 806–13.

39 Kornblau SM, Singh N, Qiu Y, Chen W, Zhang N, Coombes KR. Highly phosphorylated FOXO3A is an adverse prognostic factor in acute myeloid leukemia. *Clin Cancer Res* 2010; **16**: 1865–74.

40 Yan F, Liao R, Lin S, Deng X, Little PJ, Zheng W. Forkhead box protein O3 suppresses uveal melanoma development by increasing the expression of Bcl2like protein 11 and cyclindependent kinase inhibitor 1B. *Mol Med Rep* 2018; **17** (2): 3109–14.

41 Chou CC, Lee KH, Lai IL *et al.* AMPK reverses the mesenchymal phenotype of cancer cells by targeting the Akt-MDM2-Foxo3a signaling axis. *Cancer Res* 2014; **74** (17): 4783–95.

42 Padmaja Divya S, Pratheeshkumar P, Son YO *et al.* Arsenic induces insulin resistance in mouse adipocytes and Myotubes via oxidative stress-regulated mitochondrial Sirt3-FOXO3a signaling pathway. *Toxicol Sci* 2015; **146** (2): 290–300.

43 Peserico A, Chiacchiera F, Grossi V *et al.* A novel AMPK-dependent FoxO3A-SIRT3 intramitochondrial complex sensing glucose levels. *Cell Mol Life Sci* 2013; **70** (11): 2015–29.

44 Schumacker PT. SIRT3 controls cancer metabolic reprogramming by regulating ROS and HIF. *Cancer Cell* 2011; **19** (3): 299–300.

45 Li R, Quan Y, Xia W. SIRT3 inhibits prostate cancer metastasis through regulation of FOXO3A by suppressing Wnt/beta-catenin pathway. *Exp Cell Res* 2018; **364** (2): 143–51.

46 Wei L, Zhou Y, Qiao C *et al.* Oroxylin A inhibits glycolysis-dependent proliferation of human breast cancer via promoting SIRT3-mediated SOD2 transcription and HIF1α destabilization. *Cell Death Dis* 2015; **6**: e1714.

47 Wang S, Zhang C, Niyazi S *et al.* A novel cytoprotective peptide protects mesenchymal stem cells against mitochondrial dysfunction and apoptosis induced by starvation via Nrf2/Sirt3/FoxO3a pathway. *J Transl Med* 2017; **15** (1): 33.

48 Dehner M, Hadjihannas M, Weiske J, Huber O, Behrens J. Wnt signaling inhibits Forkhead box O3a-induced transcription and apoptosis through up-regulation of serum- and glucocorticoid-inducible kinase 1. *J Biol Chem* 2008; **283** (28): 19201–10.